SCIENTIFIC REPORTS

OPEN

Received: 21 March 2016
Accepted: 16 May 2016
Published: 06 June 2016

Photoelectrochemical Immunosensor for Detection of Carcinoembryonic Antigen Based on 2D TiO_2 Nanosheets and Carboxylated Graphitic Carbon Nitride

Huan Wang[1], Yaoguang Wang[1], Yong Zhang[1], Qi Wang[2], Xiang Ren[1], Dan Wu[1] & Qin Wei[1]

Carcinoembryonic antigen (CEA) was used as the model, an ultrasensitive label-free photoelectrochemical immunosensor was developed using 2D TiO_2 nanosheets and carboxylated graphitic carbon nitride (g-C_3N_4) as photoactive materials and ascorbic acid as an efficient electron donor. 2D TiO_2 nanosheets was sythsized by surfactant self-assembly method and proved to have higher photoelectrochemical signals than TiO_2 nanoparticles. Firstly, carboxylated g-C_3N_4 could be attached to 2D TiO_2 nanosheets through the bond formed between carboxyl group of carboxylated g-C_3N_4 and TiO_2. And the photocurrent of g-C_3N_4/TiO_2 drastically enhances compared to carboxylated g-C_3N_4 and TiO_2. Then, antibody of CEA was bonded to TiO_2 through the dentate bond formed between carboxyl group of anti-CEA and TiO_2, leading to the decrease of the photocurrents. As proven by PEC experiments and electrochemical impedance spectroscopy (EIS) analysis, the fabrication process of the immunosensor is successful. Under the optimal conditions, the intensity decreased linearly with CEA concentration in the range of 0.01~10 ng/mL. The detection limit is 2.1 pg/mL. The work provides an effective method for the detection of tumor markers and can be extended for the application in food safety and environmental monitoring analysis.

Photoelectrochemical (PEC) sensors are fabricated on photoactive electrodes which can convert photoirradiation to electrical signal. Therefore, photoactive materials are crucial for the performance of the PEC sensors. Many photoactive materials are metal-contained semiconductors, such as TiO_2, CdSe, CdTe, ZnO, ZnS, etc[1–9]. Among them, titanium dioxide is one of the most commonly employed materials because of its nontoxicity, low-cost and brilliant photochemical and chemical stability. Nevertheless, due to a wide energy band gap of 3.0 eV, TiO_2 can only absorb the ultraviolet light (<387 nm)[10]. So applications of pure TiO_2 are also limited. Another class of photoactive materials is metal-free polymeric semiconductor. Graphitic carbon nitride (g-C_3N_4), a moderate energy bandgap of 2.7 eV, has paid more and more attentions because it is very stable in acid or alkaline electrolytes[11]. However, applications of pure g-C_3N_4 are also limited largely because of its low quantum efficiency and high electron−hole recombination rate. As mentioned above, researchers have therefore made great efforts to expand the application of pure TiO_2 and pure g-C_3N_4 by various methods, such as coupling it with other materials, nanostructuring and doping[12–13]. Thus, owing to the proper band level between g-C_3N_4 and TiO_2, g-C_3N_4 and TiO_2 are combined together leading to the easy separation of the photo-generated electron and hole. Although there are some references about the combination of g-C_3N_4 and TiO_2, the morphology of TiO_2 is maily focused on nanorod[10,14], nanoparticles[11] and nanotube[15–17].

[1]Key Laboratory of Chemical Sensing & Analysis in Universities of Shandong, School of Chemistry and Chemical Engineering, University of Jinan, Jinan 250022, China. [2]School of Material Science and Engineering, University of Jinan, Jinan 250022, P.R. China. Correspondence and requests for materials should be addressed to D.W. (email: wudan791108@163.com)

Herein, two-dimensional (2D) TiO_2 nanosheets was prepared by forming inverse lamellar micelles of Pluronic P123 surfactant together with ethylene glycol (EG) co-surfactant in ethanol solvent. It is reported that 2D nanostructures exhibit superior catalytic, photovoltaic and electrochemical performances, due to their large surface-to-volume ratio and confined thickness on the atomic scale[18]. So they could have promising applications in sensors, and energy conversion and storage devices. Using carcinoembryonic antigen (CEA) as a model analyte, we developed a label-free photoelectrochemical immunosensor for detection of CEA based on 2D TiO_2 nanosheets and carboxylated graphitic carbon nitride. CEA, a usual tumor marker, can be used for the early detection of recurrent diseases and indicate the effect of therapy in early breast cancer and gastrointestinal cancers as well as other tumor markers[19,20]. Coupling carboxylated graphitic carbon nitride with 2D TiO_2 nanosheets can evidently extend the absorption range, increase the utilization of light energy, and promote the photocurrent intensity. Then, antibody of CEA was immobilized through the dentate bond formed between carboxyl group of anti-CEA and TiO_2, leading to the decrease of the PEC signal. The decreased signal is proportional to the logarithm of CEA concentration. The CEA immunosensor exhibits high sensitivity, good selectivity and wide linear range.

Experimental

Materials and reagents. Titanium isopropoxide (TTIP, 95%), ethylene glycol (EG) and ascorbic acid were purchased from Sinopharm Chemical Reagent Co., Ltd. (China). The CEA and corresponding antibody were purchased from Beijing Dingguo Changsheng Biotechnology Co. Ltd. (China). Bovine serum albumin (BSA, 96–99%) were purchased from Sigma-Aldrich (Beijing, China). All other chemicals were of analytical grade and used without further purification. ITO glass (resistivity 10 Ω/sq) is obtained from Zhuhai Kaivo Electronic Components Co. Ltd., China.

Apparatus. The scanning electron microscope (SEM) images were obtained by the field emission SEM (ZEISS, Germany). Photoelectrochemical (PEC) measurements were performed on an electrochemical workstation (Zahner Zennium PP211, Germany).

Synthesis of TiO_2 nanosheet. TiO_2 was prepared according to the literature[18,21]. 1.05 g TTIP was added into 0.74 g concentrated HCl solution under vigorous stirring (solution A); and 0.2 g Pluronic P123 was dissolved in 3.0 g ethanol (solution B) under stirring for 15 min. Then, solution B was added into solution A and stirred for another 30 min. Subsequently, 2.5 mL TTIP solution with 20 mL EG was transferred into an autoclave and heated at 150 °C for 20 h. After cooled to room temperature naturally, the resulting solid powder was collected by centrifugation and washed with ethanol several times. The final products were then dried at 80 °C for 24 h.

Synthesis of carboxylated g-C_3N_4. Carboxylated g-C_3N_4 was prepared as described previously with our reference[22]. In brief, 5.0 g of white melamine powder was put into a covered ceramic crucible and heated at 550 °C for 4 h in a muffle furnace. The yellow g-C_3N_4 product was ground to powder after cooling to room temperature. Then, 1 g g-C_3N_4 powder was placed into 100 mL 5 mol/L HNO_3 and refluxed for 24 h at 125 °C. After cooling to room temperature, the refluxed product was centrifuged and washed with water until pH reached 7. Finally, the resulting product was dried at 35 °C for 12 h in vacuum.

Synthesis of carboxylated g-C_3N_4/TiO_2 solution. In brief, 0.5 mg carboxylated g-C_3N_4 powder was dispersed in 5 mL water by ultrasonication for over 2 h. Then, 20 mg TiO_2 powder was added to the above suspension and stirred for 24 h. After that, the solution was centrifugated and the products were redispersed in 5 mL of water.

Fabrication of PEC immunosensor. The illustration of PEC immunosensor fabrication process is depicted in Fig. 1. ITO slices ($3 \times 0.5\,cm^2$) were sonicated in acetone, ethanol and water consecutively for 30 min and dried under a N_2 stream. 6 μL of carboxylated g-C_3N_4/TiO_2 solution was dropped on the surface of the pre-cleaned ITO and dried after air drying, the film was sintered at 450 °C for 30 min and then cooled down to the room temperature. Then, 4 μL of 10 μg/mL anti-CEA solution was bonded onto TiO_2 for 1 h via the bond formed between carboxyl group of anti-CEA and TiO_2 at 4 °C for 1 h[23,24]. The unreacted active sites on the electrode surface were deactivated by 6 μL of 1% bovine serum albumin (BSA) solution for 1 h. Finally, 6 μL of CEA solutions with different concentrations were incubated for 1 h the electrode was incubated with different concentration of CEA for 1 h min at 4 °C and then washed with buffer solution to remove the excess CEA. Thus, the PEC immunosensor was fabricated completely and was ready to be used.

PEC measurements. Photocurrent was measured by the current–time curve experimental technique on a photoelectrochemical workstation at a bias voltage of 0.1 V with light intensity of 150 W/cm^2. All experiments were carried out using a conventional three electrodes system with a modified ITO as working electrode, a Pt wire as counter electrode, and a saturated Ag/AgCl electrode as reference electrode.

Results and Discussion

Characterization of TiO_2 nanosheet. SEM images were used to confirm the successful synthesis of nanomaterials with different morphology. Figure 2 show the SEM images of TiO_2 (A) and carboxylated g-C_3N_4 (B). Obviously, TiO_2 exists in the form of groups of nanosheets. And the prepared carboxylated g-C_3N_4 also has the nanosheet structure.

Characterization of the immunosensor. Electrochemical impedance spectroscopy (EIS), a useful tool for evaluating electron transfer resistance, was used to monitor the stepwise modification of the electrodes. The semicircle diameter corresponds to the electron transfer resistance (Ret), which reflects the restricted diffusion of

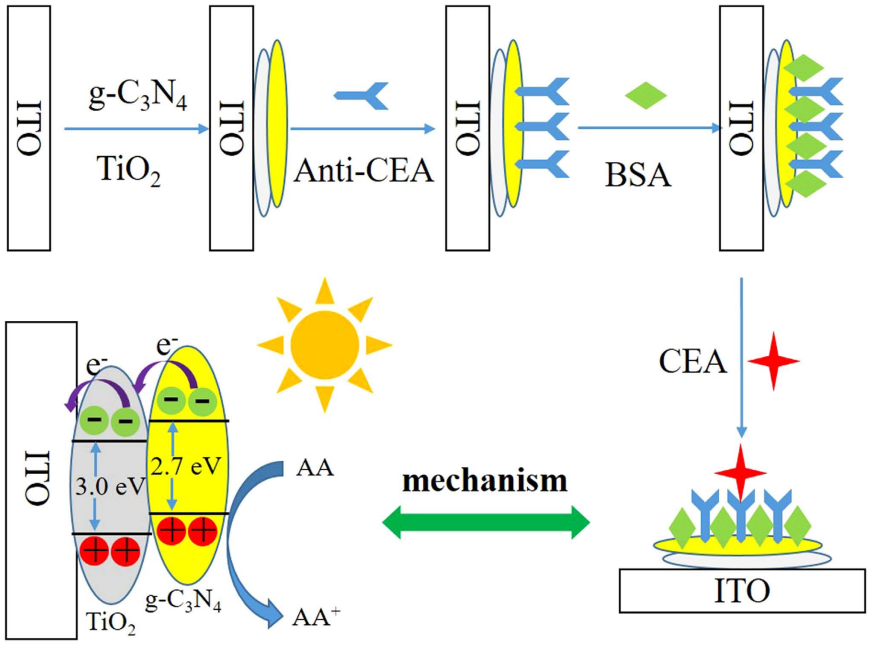

Figure 1. The illustration of PEC immunosensor fabrication process.

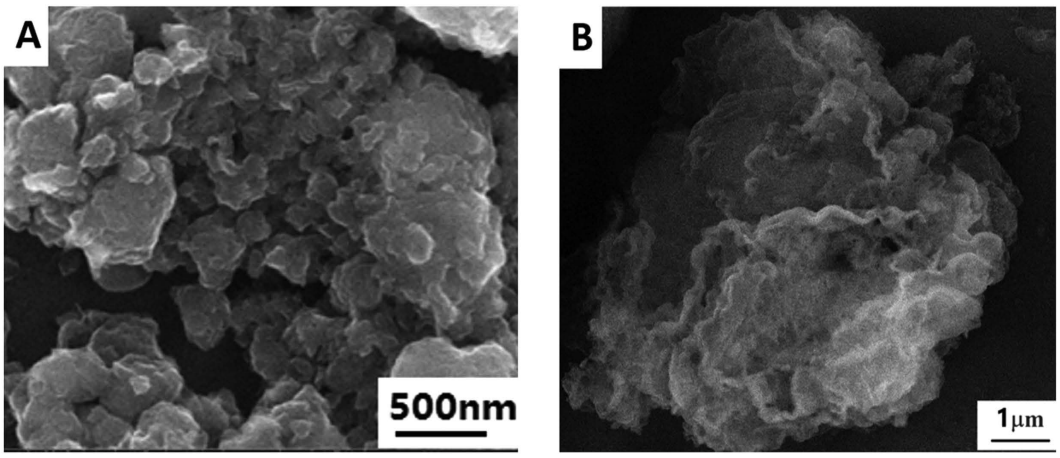

Figure 2. SEM of TiO_2 nanosheets (**A**) and carboxylated g-C_3N_4 (**B**).

the redox probe accessing the layer[25]. The measurements were carried out in 5.0 mmol/L $[Fe(CN)_6]^{3-/4-}$ solution containing 0.1 mol/L KCl and the result were shown in Fig. 3A. Non-modified ITO electrode showed a small semicircle diameter (curve a), implying a low electron transfer resistance. After coating of carboxylated g-C_3N_4/TiO_2 composite (curve b), semicircle diameter increases gradually because both carboxylated g-C_3N_4 and TiO_2 as semiconductors evidently reduced the ability of the redox probe to access the electrode surface. The sequential immobilization of CEA antibody (curve c), BSA (curve d) and CEA (curve e) led to gradual increase of the electron transfer resistance because of the insulation properties of protein.

In order to further confirm that the electrode was modified successfully, the stepwise fabrication process of the immunosensor was also characterized by PEC measurements, as shown in Fig. 3B. Compared with the ITO (curve a), the photocurrent response (curve b) was enhanced greatly after carboxylated g-C_3N_4/TiO_2 composite was immobilized on it subsequently, suggesting that carboxylated g-C_3N_4/TiO_2 have good PEC properties. With the loading of CEA antibody (curve c), BSA (curve d) and CEA (curve e) onto the modified electrode surface successively, the photocurrent intensity decreased which could be attributed to the block of biomacromolecules. Both the above results were consistent with the fact that the electrode was modified as expected.

The mechanism of electron transfers in g-C_3N_4/TiO_2 PEC immunosensor in ascorbic acid (AA) electrolyte probably is that high electron−hole recombination rate in g-C_3N_4 results in low PEC activity, when g-C_3N_4/TiO_2 composites are exposure, the photo-generated electrons from g-C_3N_4 can transfer from conduction band of g-C_3N_4 to the conduction band of TiO_2. Because the conduction band and valence band edges of g-C_3N_4 are higher than those of TiO_2 nanosheets, the above transfer process of photo-generated carriers is easy. AA is a kind

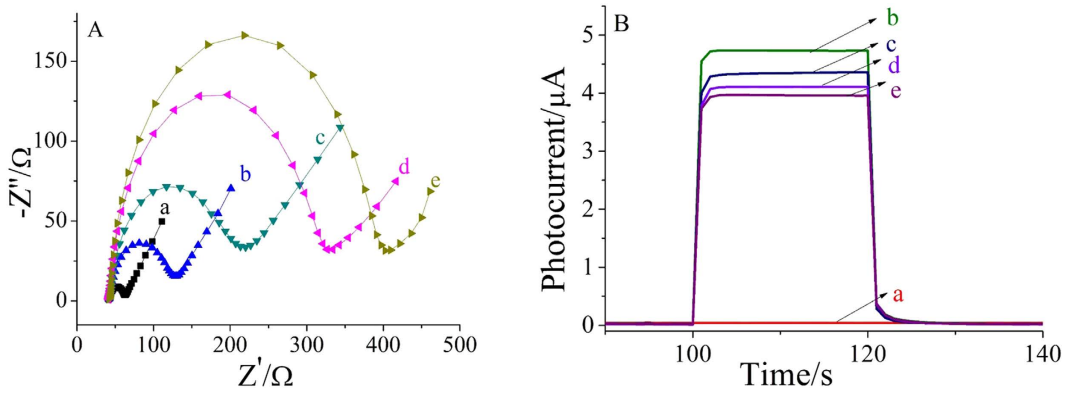

Figure 3. EIS in the presence of 5.0 mmol/L $[Fe(CN)_6]^{3-/4-}$ solution containing 0.1 mol/L KCl (**A**) and photocurrent–time curves in 0.1 mol/L PBS (pH = 7.0) containing 0.1 mmol/L AA with 0.1 V applied potential and 430 nm excitation light. (**B**) (a) ITO (b) ITO/g-C_3N_4/TiO_2 composite (c) ITO/g-C_3N_4/TiO_2/Anti-CEA (d) ITO/g-C_3N_4/TiO_2/Anti-CEA/BSA (e) ITO/g-C_3N_4 /TiO_2/Anti-CEA/BSA/CEA.

of excellent electron donor, which could block the recombination of photo-generated electrons and holes and meanwhile promote the electron transfer from conduction band of TiO_2 nanosheets to the ITO electrode. The specific binding of CEA to its antibody blocked the electron transfer from AA to g-C_3N_4/TiO_2 composite, resulting in the recombination of photo-generated holes and electrons, which could explain a decrease in photocurrent. Moreover, the photocurrent intensity decreased gradually with the increase of CEA concentration. Therefore, the quantitative detection of CEA is achieved by monitoring the photocurrent decrease after the binding of CEA.

Optimization of experimental conditions. As shown in Fig. 4A, no PEC signal were found for the ITO (curve a). Compared with the ITO, the PEC signal changed only a little after modified with g-C_3N_4 (curve b) due to the low quantum efficiency and high electron−hole recombination rate of g-C_3N_4. Moreover, TiO_2 showed obvious PEC signal, and the photocurrent intensity of TiO_2 nanosheets (curve d) was 30% higher than that of TiO_2 nanoparticles (curve c). It illustrates that TiO_2 with different morphology has different photoelectric response performance, and nanosheet is superior to nanoparticles in this system. Although pure g-C_3N_4 did not show obvious PEC signal, but when it was combined with TiO_2, the PEC signal was significantly increased (curve e), which was 12% higher than that of pure TiO_2 nanosheets and much larger than the sum of the two kinds of nanomaterials, suggesting there is energy level matching between g-C_3N_4 and TiO_2. This is the reason why both carboxylated g-C_3N_4 and TiO_2 were chosen as photoactive materials.

To obtain an optimal PEC signal, pH value of substrate solution was investigated. Keeping the concentrations of CEA constant, the effect of pH on the photocurrent intensity was studied over a pH range from 5.0–8.0, as shown in Fig. 4B. The photocurrent intensity increased with the increase of pH from 5.0–7.0 and reached the maximum. After that, the photocurrent intensity decreased accordingly with pH increasing from 7.0–8.0. This suggests that the neutral condition is more advantageous to the photoelectric response of the carboxylated g-C_3N_4 and TiO_2 nanosheets system. Therefore, pH 7.0 was chosen as the optimal value.

The effect of TiO_2 concentration was also tested. As shown in Fig. 4C, the photocurrent intensity increased when TiO_2 concentration increased from 1 to 4 mg/mL because more photoactive materials are formed and light absorption is enhanced. After that, the photocurrent intensity is decreased because thicker C_3N_4/TiO_2 film could also lead to increased diffusion resistance for electron motion. Thus, 4 mg/mL TiO_2 was chosen for subsequent study.

The concentration of AA as an efficient electron donor was evaluated to improve the photocurrent response of the PEC sensor. It can be seen from Fig. 4D that the photocurrent intensity reached a maximum value at 0.1 mol/L AA. Thus, 0.1 mol/L AA PBS solution (pH 7.0) was used as the buffer electrolyte for CEA detection.

Under the optimal conditions, a series of photoelectrochemical immunosensors were incubated with different concentrations of CEA and subsequent determination was carried out. As expected, the photocurrents decreased with the increase of CEA concentration due to the biomolecular insulation properties of CEA. Moreover, it can be seen from Fig. 5 that the photocurrent intensity decreased linearly with CEA concentration in the range from 0.01–10 ng/mL with a detection limit of 2.1 pg/mL (S/N = 3). Table 1 shows the comparison of the proposed photoelectrochemical immunosensors with other previously reported immunosensors for the detection of CEA[26–30]. As seen from the table, the detection limit of this work are superior to the previously reported immunosensors, indicating that the proposed PEC immunosensor has a good performance.

Stability and Selectivity. The stability of the designed immunosensor was also evaluated by using a prepared PEC immunosensor for the detection of 5 ng/mL CEA. The photocurrent responses were recorded under several on/off irradiation cycles for 550 s. As shown in Fig. 6A, there was only a little change of the photocurrent, indicating the developed PEC sensors have stable photocurrent response for CEA detection.

Figure 6B shows the selectivity test of the ECL immunosensor for 5 ng/mL CEA. The photocurrents were measured by mixing 5 ng/mL of CEA with 50 ng/mL prostate-specific antigen (PSA), 50 ng/mL human immune globulin G (H-IgG), 50 ng/mL BSA and 50 ng/mL glucose, respectively. The photocurrent exhibited no obvious

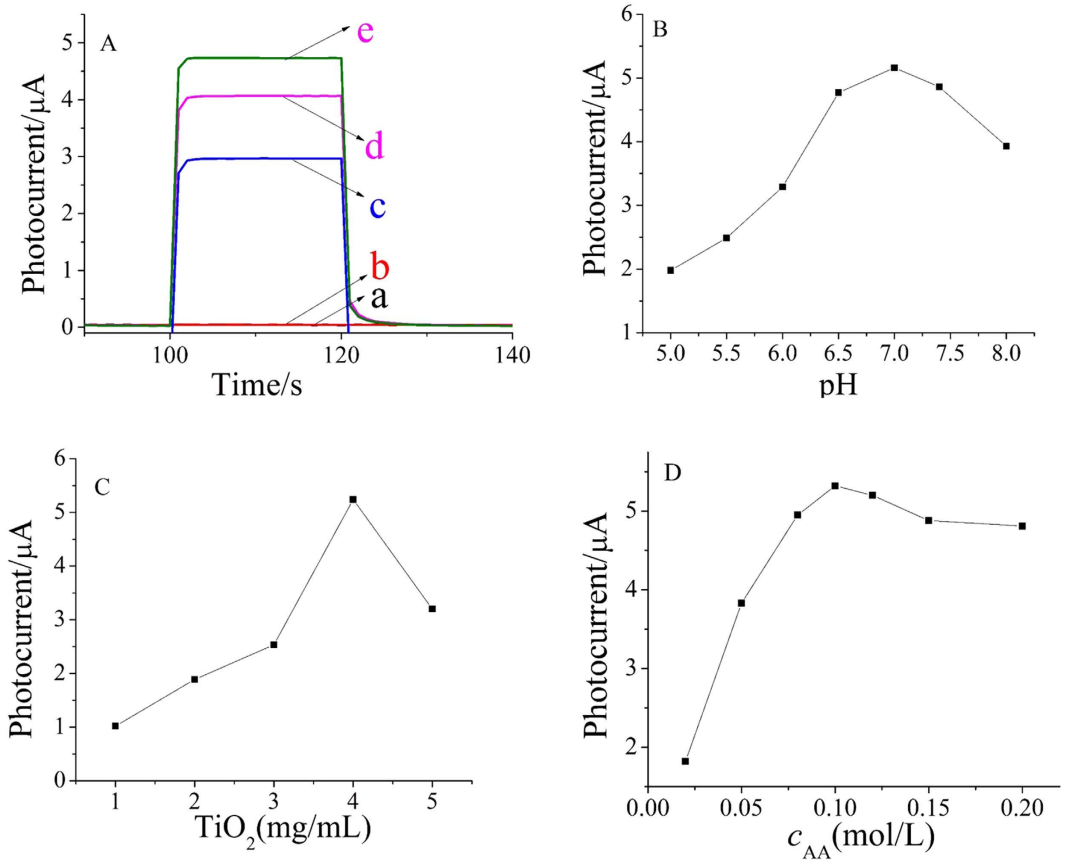

Figure 4. Photocurrent responses of different modified materials (**A**) effect of pH (**B**) the concentration of TiO_2 (**C**) and the concentration of AA (**D**) on the photocurrent intensity. (a) ITO (b) ITO/g-C_3N_4 (c) ITO/TiO_2 nanoparticles (d) ITO/TiO_2 nanosheets (e) ITO/g-C_3N_4/TiO_2 composite.

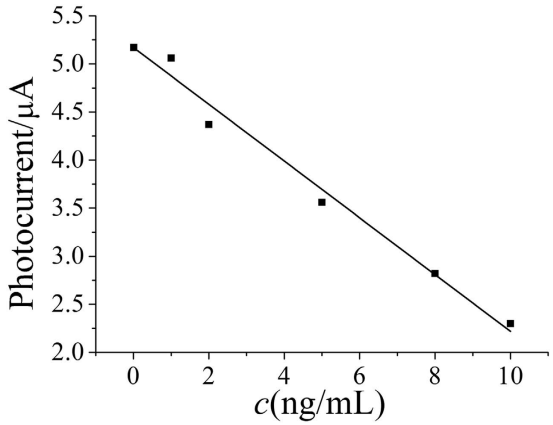

Figure 5. Calibration curve of the immunosensor for different concentrations of CEA.

change compared with the 5 ng/mL of CEA, which indicated excellent selectivity and specificity of the PEC immunosensor for CEA.

Serum sample analysis. The amount of CEA was measured 5 times in human serum sample and the relative standard deviation (RSD) was calculated to obtain the precision. The accuracy was also studied through a recovery experiment using standard addition method. 1.00 ng/mL CEA standard solution was added to the corresponding samples. With the same experiments measured for five times, the average recovery was calculated. It can be found from Table 2 that the relative standard deviation is 3.1% and the recovery is 99.2%. Hence, the proposed immunosensor can be used for CEA detection with satisfied results.

Materials	Detection ranges (ng/mL)	Detection limits (ng/mL)	References
CS–CNTs–GNPs nanocomposite film	0.1–2.0	0.04	26
[Ag–Ag_2O]/SiO_2 nanocomposite material	0.5–160	0.14	27
Thi@NPG/AuNPs	0.01–100	0.003	28
AuNP@nafion/FC@CHIT	0.01–150	0.0031	29
HRP-anti-CEA-NGGN	0.05–350	0.01	30
Carboxylated g-C_3N_4/TiO_2 nanosheets	0.01–10	0.0021	This work

Table 1. Comparison with other previously reported immunosensors for the detection of CEA.

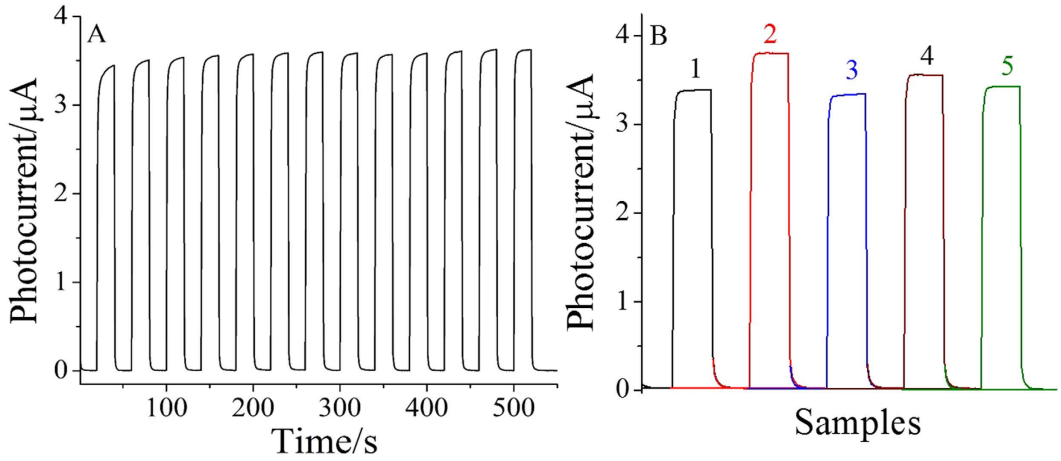

Figure 6. The stability of the immunosensor incubated with 5 ng/mL CEA under several on/off irradiation cycles for 550 s (**A**) and the selectivity of the immunosensor (**B**). 5 ng/mL CEA (1), 5 ng/mL CEA + 50 ng/mL PSA (2), 5 ng/mL CEA + 50 ng/mL H-IgG (3), 5 ng/mL CEA + 50 ng/mL BSA (4), 5 ng/mL CEA + 50 ng/mL glucose (5).

Sample	Content of PSA (ng/mL)	Average ($n = 5$, ng/mL)	RSD (%)	Added (ng/mL)	Recovery value (ng/mL)	Recovery ($n = 5$, ng/mL)
Human serum	1.35	1.39	3.1	1.00	1.03	99.2
	1.42			1.00	0.95	
	1.45			1.00	1.01	
	1.37			1.00	0.92	
	1.36			1.00	1.05	

Table 2. Results for the determination of CEA in human serum sample.

Conclusions

This work demonstrated a label-free photoelectrochemical immunosensor for detection of carcinoembryonic antigen using carboxylated g-C_3N_4 and 2D TiO_2 nanosheets as photoactive materials. 2D TiO_2 nanosheets exhibits better photocatalytic activities than TiO_2 nanoparticles and g-C_3N_4 can improve its photocatalytic performance due to the good energy level matching. Great photocatalytic activities of g-C_3N_4/TiO_2 nanosheets together with the specificity of immunoreaction made sensitive detection of CEA possible. The proposed immunosensor has excellent performance with high sensitivity, good selectivity and stability. Moreover, this strategy could be used to develop photoelectrochemical immunosensors for other targets.

References

1. Zang,Y., Lei, J., Hao, Q. & Ju, H. CdS/MoS_2 heterojunction-based photoelectrochemical DNA biosensor via enhanced chemiluminescence excitation. *Biosens. Bioelectron.* **77,** 557–564 (2016).
2. Fan, G. C., Han, L., Zhu, H., Zhang, J. R. & Zhu, J. J. Ultrasensitive photoelectrochemical immunoassay for matrix metalloproteinase-2 detection based on CdS:Mn/CdTe cosensitized TiO_2 nanotubes and signal amplification of SiO_2@Ab_2 conjugates. *Anal. Chem.* **86,** 12398–12405 (2014).
3. Li, W. *et al.* Stable core/shell CdTe/Mn-CdS quantum dots sensitized three-dimensional, macroporous ZnO nanosheet photoelectrode and their photoelectrochemical properties. *ACS Appl. Mater. Interfaces*, **6,** 12353–12362 (2014).
4. Zhou, S., Wang, Y., Zhao, M., Jiang, L. P. & Zhu, J. J. CdSeTe@CdS@ZnS quantum-dot-sensitized macroporous TiO_2 film: a multisignal-amplified photoelectrochemical platform. *ChemPhysChem* **16,** 2826–2835 (2015).
5. Han, J. *et al.* Synthesis of metal sulfide sensitized zinc oxide-based core/shell/shell nanorods and their photoelectrochemical properties. *J. Power Sources* **268,** 388–396 (2014).

6. Neto, S. Y., Luz, R. C. S. & Damos, F. S. Visible LED light photoelectrochemical sensor for detection of L-Dopa based on oxygen reduction on TiO_2 sensitized with iron phthalocyanine. *Electrochem. Commun.* **62,** 1–4 (2016).
7. Moakhar, R. S., Goh, G. K. L., Dolati, A. & Ghorbani, M. A novel screen-printed TiO_2 photoelectrochemical sensor for direct determination and reduction of hexavalent chromium. *Electrochem. Commun.* **61,** 110–113 (2015).
8. Xin, Y., Li, Z. & Zhang, Z. Photoelectrochemical aptasensor for the sensitive and selective detection of kanamycin based on Au nanoparticle functionalized self-doped TiO_2 nanotube arrays. *Chem. Commun.* **51,** 15498–15501 (2015).
9. Wang, M. *et al.* Visible-light induced photoelectrochemical biosensor for the detection of microRNA based on Bi_2S_3 nanorods and streptavidin on an ITO electrode. *Microchim. Acta* **182,** 241–248 (2015).
10. Li, Y. *et al.* Efficient and stable photoelectrochemical seawater splitting with TiO_2@g-C_3N_4 nanorod arrays decorated by Co-Pi. *J. Phys. Chem. C* **119,** 20283–20292 (2015).
11. Cai, Z. *et al.* Solar-induced photoelectrochemical sensing for dopamine based on TiO_2 nanoparticles on g-C_3N_4 decorated graphene nanosheets. *J. Electroanal. Chem.* **759,** 32–37 (2015).
12. Yin, H. *et al.* Photoelectrochemical immunosensor for microRNA detection based on gold nanoparticles-functionalized g-C_3N_4 and anti-DNA: RNA antibody. *Sens. Actuators B* **222,** 1119–1126 (2016).
13. Hou, Y., Wen, Z., Cui, S., Guo, X. & Chen, J. Constructing 2D porous graphitic C_3N_4 nanosheets/nitrogen-doped graphene/layered MoS_2 ternary nanojunction with enhanced photoelectrochemical activity. *Adv. Mater.* **25,** 6291–6297 (2013).
14. Wang, J. & Zhang, W. D. Modification of TiO_2 nanorod arrays by graphite-like C_3N_4 with high visible light photoelectrochemical activity. *Electrochim. Acta* **71,** 10–16 (2012).
15. Liu, L., Zhang, G., Irvine, J. T. S. & Wu, Y. Organic semiconductor g-C_3N_4 modified TiO_2 nanotube arrays for enhanced photoelectrochemical performance in wastewater treatment. *Energy Technol.* **3,** 982–988 (2015).
16. Yang, M. *et al.* C_3N_4-sensitized TiO_2 nanotube arrays with enhanced visible-light photoelectrochemical performance. *Phys. Chem. Chem. Phys.* **17,** 17887–17893 (2015).
17. Zhang, Y. *et al.* Synthesis of g-C_3N_4/Bi_2O_3/TiO_2 composite nanotubes: enhanced activity under visible light irradiation and improved photoelectrochemical activity. *RSC Adv.* **5,** 48983–48991 (2015).
18. Sun, Z. *et al.* Generalized self-assembly of scalable two-dimensional transition metal oxide nanosheets. *Nat. Commun.* **5,** 3813–3821 (2014).
19. Zhang, K. *et al.* A long way to go for the harmonization of four immunoassays for carcinoembryonic antigen. *Clin. Chim. Acta* **454,** 15–19 (2016).
20. Gao, Y. S. *et al.* Label-free electrochemical immunosensor based on Nile blue A-reduced graphene oxide nanocomposites for carcinoembryonic antigen detection. *Anal. Biochem.* doi: 10.1016/j.ab.2016.02.010 (2016).
21. Xin, Y. *et al.* Gold–palladium bimetallic nanoalloy decorated ultrathin 2D TiO_2 nanosheets as efficient photocatalysts with high hydrogen evolution activity. *J. Mater. Chem. A* **3,** 8659–8666 (2015).
22. Li, X. *et al.* Cathodic electrochemiluminescence immunosensor based on nanocomposites of semiconductor carboxylated g-C_3N_4 and graphene for the ultrasensitive detection of squamous cell carcinoma antigen. *Biosens. Bioelectron.* **55,** 330–336 (2014).
23. Tu, W., Lei, J., Ding, L. & Ju, H. Sandwich nanohybrid of single-walled carbon nanohorns–TiO_2–porphyrin for electrocatalysis and amperometric biosensing towards chloramphenicol. *Chem. Commun.* **28,** 4227–4229 (2009).
24. Gao, P. *et al.* Construction of dentate bonded TiO_2–CdSe heterostructures with enhanced photoelectrochemical properties: versatile labels toward photoelectrochemical and electrochemical sensing. *Dalton Trans.* **44,** 773–781 (2015).
25. Fan, G. C., Han, L., Zhang, J. R. & Zhu, J. J. Enhanced Photoelectrochemical strategy for ultrasensitive DNA detection based on two different sizes of CdTe quantum dots cosensitized TiO_2/CdS:Mn hybrid structure. *Anal. Chem.* **86,** 10877–10884 (2014).
26. Gao, X. *et al.* One step electrochemically deposited nanocomposite film of chitosan–carbon nanotubes–gold nanoparticles for carcinoembryonic antigen immunosensor application. *Talanta* **85,** 1980–1985 (2011).
27. Yuan, Y. *et al.* A novel label-free electrochemical immunosensor for carcinoembryonic antigen detection based on the [Ag–Ag_2O]/SiO_2 nanocomposite material as a redox probe. *J. Electroanal. Chem.* **643,** 15–19 (2010).
28. Sun, X. & Ma, Z. Electrochemical immunosensor based on nanoporpus gold loading thionine for carcinoembryonic antigen. *Anal. Chim. Acta* **780,** 95–100 (2013).
29. Shi, W. & Ma, Z. A novel label-free amperometric immunosensor for carcinoembryonic antigen based on redox membrane. *Biosens. Bioelectron.* **26,** 3068–3071 (2011).
30. Zhong, Z. *et al.* Nanogold-enwrapped graphene nanocomposites as trace labels for sensitivity enhancement of electrochemical immunosensors in clinical immunoassays: Carcinoembryonic antigen as a model. *Biosens. Bioelectron.* **25,** 2379–2383 (2010).

Acknowledgements

This study was supported by the Natural Science Foundation of China (No. 21377046, 21405059 and 21575050), Shandong Province (No. ZR2014BL024) and University of Jinan (No. XKY1405). Qin Wei thanks the Special Foundation for Taishan Scholar Professorship of Shandong Province and University of Jinan (No. ts20130937).

Author Contributions

H.W. and D.W. conceived and designed the experiments. H.W., Y.W. and Y.Z. performed the experiments, analyzed the data and wrote the first draft of the manuscript. Q.W., X.R. and Q.W. contributed substantially to revisions.

Additional Information

Competing financial interests: The authors declare no competing financial interests.

How to cite this article: Wang, H. *et al.* Photoelectrochemical Immunosensor for Detection of Carcinoembryonic Antigen Based on 2D TIO_2 Nanosheets and Carboxylated Graphitic Carbon Nitride. *Sci. Rep.* **6**, 27385; doi: 10.1038/srep27385 (2016).